

Article

Electrochemical Study on Newly Synthesized Chlorocurcumin as an Inhibitor for Mild Steel Corrosion in Hydrochloric Acid

Ahmed A. Al-Amiery ^{1,2,*}, Abdul Amir H. Kadhum ¹, Abu Bakar Mohamad ¹, Ahmed Y. Musa ³ and Cheong Jiun Li ¹

¹ Department of Chemical and Process Engineering, Universiti of Kebangsaan Malaysia (UKM), Bangi, Selangor 43000, Malaysia; E-Mails: amie@eng.ukm.my (A.A.H.K.); drab@eng.ukm.my (A.B.M.); jiunli@gmail.com (C.J.L.)

² Environmental Research Center, University of Technology (UOT), Baghdad 10001, Iraq

³ Department of Chemistry, Western University, 1151 Richmond Street, London, Ontario N6A3K7, Canada; E-Mail: amusa6@uwo.ca

* Author to whom correspondence should be addressed; E-Mail: dr.ahmed1975@gmail.com; Tel.: +601-6392-3439; Fax: +603-8921-6148.

Received: 2 August 2013; in revised form: 17 October 2013 / Accepted: 8 November 2013 / Published: 27 November 2013

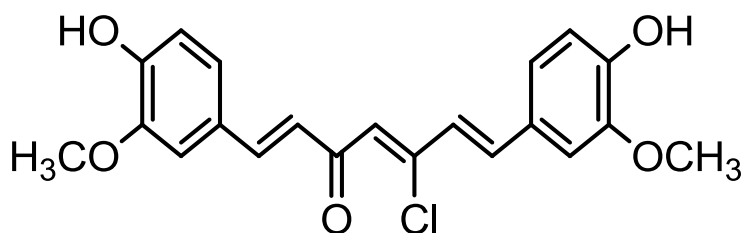
Abstract: A new curcumin derivative, *i.e.*, (1E,4Z,6E)-5-chloro-1,7-bis(4-hydroxy-3-methoxyphenyl)hepta-1,4,6-trien-3-one (chlorocurcumin), was prepared starting with the natural compound curcumin. The newly synthesized compound was characterized by elemental analysis and spectral studies (IR, ¹H-NMR and ¹³C-NMR). The corrosion inhibition of mild steel in 1 M HCl by chlorocurcumin has been studied using potentiodynamic polarization (PDP) measurements and electrochemical impedance spectroscopy (EIS). The inhibition efficiency increases with the concentration of the inhibitor but decreases with increases in temperature. The potentiodynamic polarization reveals that chlorocurcumin is a mixed-type inhibitor. The kinetic parameters for mild steel corrosion were determined and discussed.

Keywords: corrosion inhibition; chlorocurcumin; polarization; potentiodynamic

1. Introduction

Natural Products (NPs) have traditionally played an important role in industrial applications, including the discovery of drug NPs, which were the basis for most early medicines [1,2]. Many organic compounds have been studied to investigate their corrosion inhibition potential, e.g., the effect of organic nitrogen compounds on the corrosion behavior of iron and steel in acidic solutions; these organic nitrogen compounds are usually employed for their rapid action [3,4]. The effective and efficient corrosion inhibitors are those compounds that have π -bonds, contain hetero-atoms such as sulfur, nitrogen, oxygen and phosphorous and allow the adsorption of compounds on the metal surface [5–9]. The organic inhibitors decrease the corrosion rate by adsorbing on the metal surface and blocking the active sites by displacing water molecules, leading to the formation of a compact barrier film on the metal surface. Most organic inhibitors are toxic, highly expensive and environmentally unfriendly. Thermodynamic adsorption parameters and kinetic corrosion parameters have been utilized to describe inhibitor adsorption behavior. Riggs and Hurd [10] reported that the heat of inhibitor adsorption could be obtained by comparing the activation energies of uninhibited and inhibited corrosion reactions. However, while a positive heat of adsorption, differential heat of adsorption (DHads.) $\text{DHads.} > 0$ (endothermic process), has been unequivocally attributed to chemisorption, [10,11] a negative heat of adsorption, $\text{DHads.} < 0$ (exothermic process), could involve physisorption, [12] chemisorption [13,14] or a mixture of both processes (comprehensive adsorption) [14–19]. It is well established that the effect of temperature on the inhibition of an acid–metal reaction is highly complex, due to the many changes that occur on the metal surface, such as the rapid etching and desorption of the inhibitor, and because the inhibitor itself may undergo decomposition and/or rearrangement. It was observed that few inhibitors in acid-metal systems have specific reactions that are effective at high temperatures rather than at low temperatures [15]. The temperature dependence of the inhibiting effect and a comparison of the values of the apparent activation energy, E_a , of the corrosion process in the absence and presence of the inhibitor of interest could provide further evidence concerning its mechanism of inhibition [16]. In the present study, corrosion inhibitor (1E,4Z,6E)-5-chloro-1,7-bis(4-hydroxy-3-methoxyphenyl)hepta-1,4,6-trien-3-one (chlorocurcumin) was synthesized and investigated as an inhibitor for the corrosion of mild steel in 1.0 M hydrochloric acid (HCl) using electrochemical impedance spectroscopy (EIS), potentiodynamic polarization (PDP) and electrochemical frequency modulation (EFM). The structure for the synthesized novel corrosion inhibitor proposed based on spectroscopic evidence and is shown in Figure 1.

Figure 1. Structure of chlorocurcumin.



2. Results and Discussion

2.1. Polarization Measurements

The polarization curves for mild steel in 1.0 M HCl solutions at various concentrations of chlorocurcumin at 30 °C are shown in Figure 2. The values for corrosion current density (i_{corr}), corrosion potential (E_{corr}), anodic Tafel slope (β_a), cathodic Tafel slope (β_c) and inhibition efficiency ($IE\%$) are displayed in Table 1. These values were calculated from the Tafel fit routine provided by the Gamry Echem analyst software, which uses a non-linear chi-squared minimization to fit the data to the Stern-Geary equation. The inhibition efficiency was calculated as follows:

$$IE(\%) = \frac{i_{\text{corr}} - i_{\text{corr(inh)}}}{i_{\text{corr}}} \times 100 \quad (1)$$

where i_{corr} and $i_{\text{corr(inh)}}$ are the corrosion current densities without and with the addition of inhibitor, respectively.

Figure 2. Potentiodynamic polarization curves for mild steel in 1.0 M HCl at 30 °C with different concentrations of chlorocurcumin.

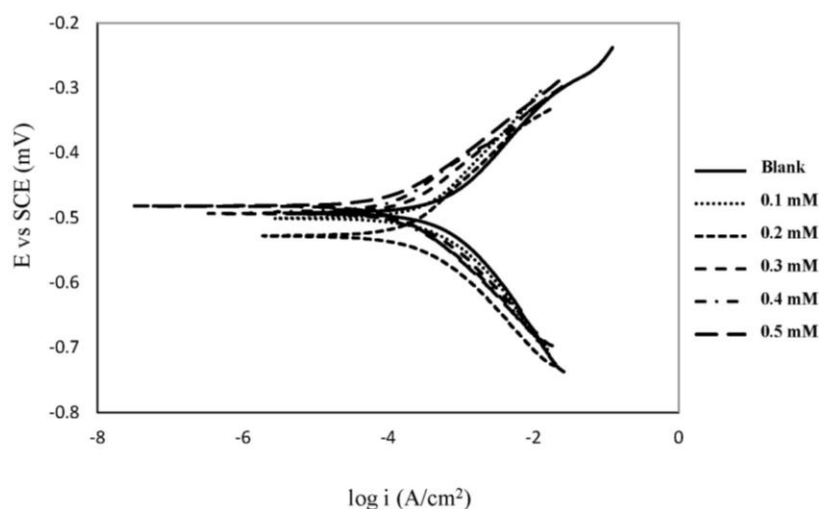


Table 1. Polarization parameters for mild steel in 1.0 M HCl with different concentrations of chlorocurcumin at 30 °C.

Concentration (mM)	β_a (V dec ⁻¹)	β_c (V dec ⁻¹)	i_{corr} ($\mu\text{A cm}^{-2}$)	$-E_{\text{corr}}$ (mV vs. SCE)	$IE\%$
Blank	0.12	0.14	660.1	491	0.00
0.1	0.15	0.13	421.0	501	36.22
0.2	0.12	0.11	254	528	61.52
0.3	0.10	0.11	232	493	64.85
0.4	0.09	0.10	150	491	77.28
0.5	0.09	0.11	145	482	78.03

A compound can be classified as an anodic- or cathodic-type inhibitor when the displacement in E_{corr} is larger than 85 mV with respect to E_{corr}^0 [20,21]. Because the largest displacement of E_{corr} occurs in the presence of chlorocurcumin, then the molecules can be considered a mixed-type inhibitor.

Adding chlorocurcumin to HCl solution reduces the anodic dissolution of mild steel and retards the cathodic hydrogen evolution.

Table 1 shows that the i_{corr} values decreased in the presence of chlorocurcumin. This result indicates that the corrosion rate decreases with the addition of inhibitor and that the inhibition efficiency increases with inhibitor concentration. The slight change in the values of the Tafel constants (β_a , β_c) with the addition of chlorocurcumin indicates that the inhibitor controlled both reactions. This result also indicates that the adsorbed molecules did not affect the mechanism of mild steel dissolution or hydrogen evolution [22].

2.2. Electrochemical Impedance Spectroscopy (EIS) Measurements

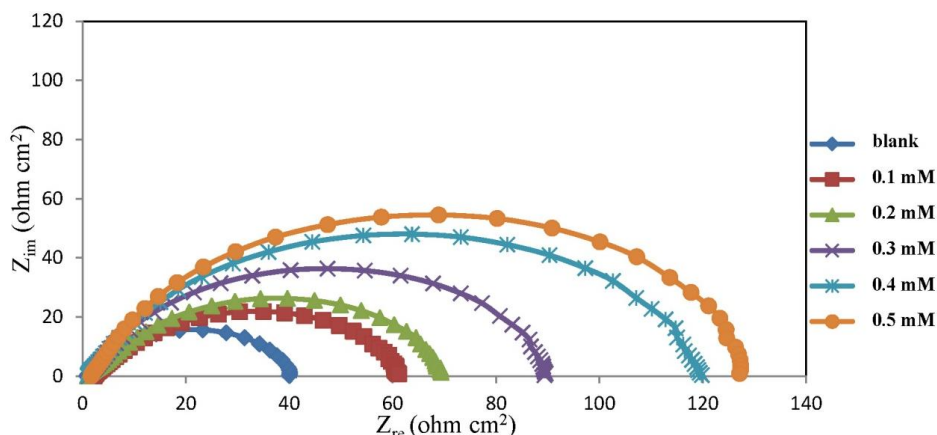
The experimental results obtained from EIS measurements for the corrosion of mild steel in the presence and absence of chlorocurcumin at 30 °C are listed in Table 2. The Nyquist plot for mild steel in the absence and presence of various concentration of chlorocurcumin is shown in Figure 3. The increase in the diameter of the semicircle indicates that impedance increases with increasing inhibitor concentration. In general, the impedance spectra exhibit one single depressed semicircle, and the diameter of the semicircle increases with the increase of inhibitor concentration. The semicircle can be attributed to the charge transfer that takes place at electrode/solution interface, and the transfer process controls the corrosion reaction of mild steel. The existence of a single semicircle shows the single charge transfer process during dissolution which is unaffected by the presence of inhibitor molecules [23,24]. The semicircle-shaped Nyquist plots imply that the formation of a barrier on the surface and the corrosion of mild steel are largely controlled by a charge transfer process [25]. The existence of single semicircle showed the single charge transfer process during dissolution which is unaffected by the presence of inhibitor molecules. Deviation of perfect circular shape is often referred to the frequency dispersion of interfacial impedance. This anomalous behavior is generally attributed to the inhomogeneity of the metal surface arising from surface roughness or interfacial phenomena [26,27]. The obtained semicircles cut the real axis at higher and lower frequencies. The intercept corresponds to R_s at the higher frequency (Table 2) end and to $R_s + R_t$ at the lower frequency end, where R_t is the difference between these two values [28].

Table 2. Impedance parameters for mild steel in 1.0 M HCl with different concentrations of chlorocurcumin at 30 °C.

Concentration (mM)	R_s (ohm cm ⁻²)	R_{ct} (ohm cm ⁻²)	$CPE_{dl} Y_0 \times 10^{-5}$ (Ss ^{α} /cm ²)	α	C_{dl} (μ F cm ⁻²)	IE%
0	–	42.00	–	0.78	294.47	0.00
0.1	2.15	61.45	60.48	0.74	190.21	31.65
0.2	0.69	87.85	47.60	0.76	174.68	52.19
0.3	1.12	91.55	38.86	0.81	177.69	54.12
0.4	0.94	121.40	27.37	0.82	159.64	65.40
0.5	1.65	130.80	29.10	0.84	126.14	67.89

Note: R_s , solution resistance; R_{ct} , charge-transfer resistance; CPE, constant phase element; α denotes an empirical parameter.

Figure 3. Nyquist plot for mild steel in 1.0 M HCl at 30 °C with different concentrations of chlorocurcumin.



The EIS spectra were analyzed using the equivalent circuit in Figure 4. The constant phase element (CPE) is represented as follows:

$$Z(\omega) = Y_o \cdot (j\omega)^{-\alpha} \tag{2}$$

where Y_o is the CPE constant, ω is the angular frequency (rad/s), $j^2 = -1$ and is an imaginary number and α is the CPE exponent. The double layer charge transfer, C_{dl} , can be calculated as follows:

$$C_{dl} = (Y_o R_{ct}^{1-\alpha})^{1/\alpha} \tag{3}$$

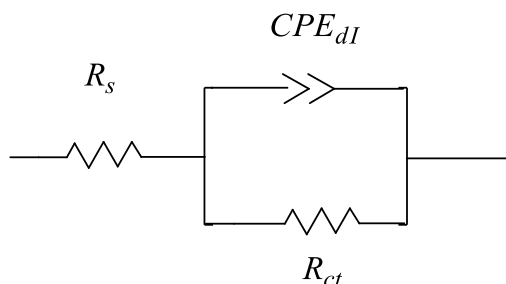
To confirm the polarization results, the inhibition efficiencies ($IE\%$) for mild steel in 1.0 M HCl is calculated as follows:

$$IE(\%) = \frac{R_{ct} - R_{ct}^o}{R_{ct}} \times 100 \tag{4}$$

where R_{ct} and R_{ct}^o are the charge transfer resistances with and without inhibitor, respectively.

The $IE\%$ increased with inhibitor concentration, and this result was in agreement with those obtained from the potentiodynamic polarization measurements. It can be observed from Table 2 that the presence of chlorocurcumin increases the values of R_{ct} and reduces the C_{dl} values. The increased R_{ct} values are due to the formation of a protective film on the metal surface that prevents mass and charge transfer [29]. Conversely, the decrease in C_{dl} is attributed to the increase in the film layer thickness formed by the adsorption of inhibitor molecules [30–32].

Figure 4. Equivalent circuit model used to fit the impedance data for mild steel.



2.3. Corrosion Kinetic Parameters

The effect of temperature on the corrosion parameter of mild steel in 1.0 M HCl was studied at 30, 40, 50 and 60 °C. The activation energy (E_a), activation enthalpy (ΔH_a) and activation entropy (ΔS_a) for the corrosion of mild steel in 1.0 M HCl with and without the inhibitor were determined using the Arrhenius and transition state plots.

The activation energy can be obtained from the Arrhenius equation and plot:

$$i_{\text{corr}} = A \exp\left(-\frac{E_a}{RT}\right) \quad (5)$$

where i_{corr} is the corrosion current (A cm^{-2}), A is pre-exponential factor, E_a is activation energy (J mol^{-1}), R is gas constant ($8.314 \text{ J mol}^{-1} \text{ K}^{-1}$) and T is temperature in K.

Taking the logarithm yields:

$$\ln i_{\text{corr}} = \left(\frac{-E_a}{R}\right)\left(\frac{1}{T}\right) + \ln A \quad (6)$$

The graph of $\ln(i_{\text{corr}})$ against $1000/T$ yields a straight line with the slope equal to $(-E_a/R)$. The Arrhenius plot for mild steel in 1.0 M HCl in the presence and absence of chlorocurcumin is shown in Figure 5. The values of E_a were calculated and are displayed in Table 3.

Figure 5. Arrhenius plot for mild steel in 1.0 M HCl.

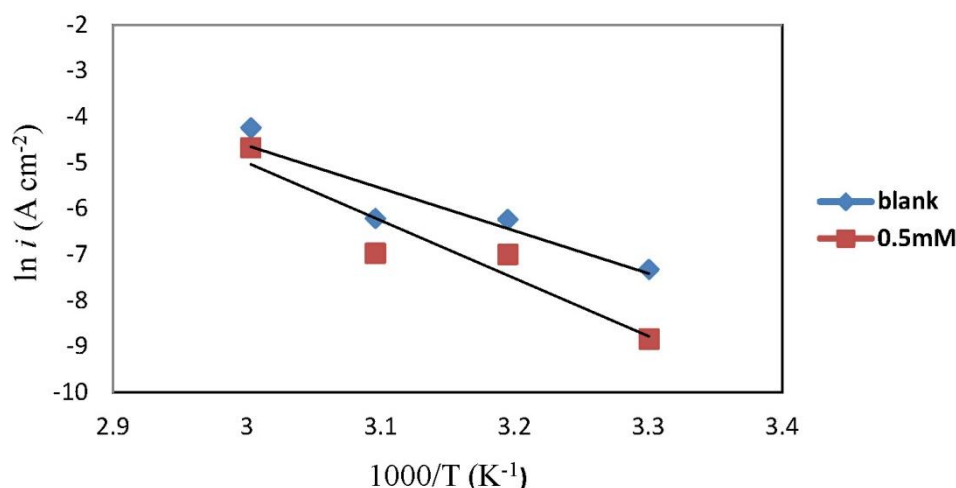


Table 3. Corrosion kinetic parameters for mild steel in 1.0 M HCl in the presence and absence of chlorocurcumin.

Concentration	E_a (kJ mol^{-1})	ΔH_a (kJ mol^{-1})	ΔS_a ($\text{J mol}^{-1} \text{ K}^{-1}$)
Blank	77.25	74.61	-60.44
0.5 mM	104.74	102.10	18.91

The transition state equation was used to calculate the ΔH_a and ΔS_a :

$$i_{\text{corr}} = \frac{RT}{hN} \exp\left(\frac{\Delta S_a}{R}\right) \exp\left(\frac{-\Delta H_a}{RT}\right) \quad (7)$$

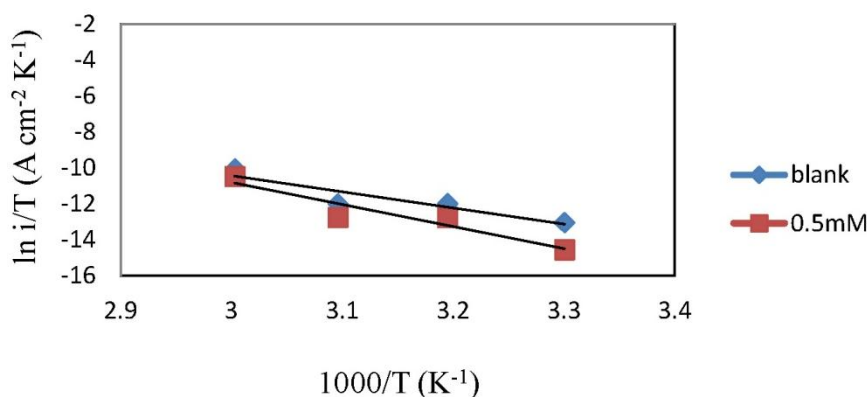
where N is Avogadro's number ($6.02 \times 10^{23} \text{ mol}^{-1}$) and h is Plank's constant ($6.63 \times 10^{-34} \text{ m}^2 \text{ kg s}^{-1}$).

To carry out simple calculations, Equation (7) was rearranged to become

$$\ln\left(\frac{i_{\text{corr}}}{T}\right) = \left(\frac{-\Delta H_a}{R}\right)\left(\frac{1}{T}\right) + \left[\ln\left(\frac{R}{Nh}\right) + \frac{\Delta S_a}{R}\right] \quad (8)$$

A plot of $\ln(i_{\text{corr}}/T)$ against $1000/T$ gives a straight line with the slope equal to $(-\Delta H_a/R)$ and intercept equal to $[\ln(R/Nh) + (\Delta S_a/R)]$, as shown in Figure 6. The ΔH_a and ΔS_a values were calculated and are displayed in Table 3.

Figure 6. Transition state plots for mild steel in 1.0 M HCl.



From Table 3, the activation energy increases in the presence of the inhibitor, implying that a physical adsorption (electrostatic) process occurred in the initial stage. In addition, the E_a values are greater than 20 kJ mol^{-1} in both the presence and absence of the inhibitor, which indicate that the entire process is controlled by the surface reaction [33]. According to Szauer and Brand, the increase in activation energy can be attributed to the decrease in the adsorption of the inhibitor on the mild steel surface with increases in temperature [34]. The values of E_a and ΔH_a are higher in the presence of the inhibitor. This result shows that the energy barrier of the corrosion reaction is increased without changing the mechanism of dissolution. The endothermic nature of steel dissolution is indicated by the positive values of ΔH_a for both the corrosion processes with and without the inhibitor.

Meanwhile, the positive values of ΔS_a reveals that the adsorption process is accompanied by an increase in the entropy which acts as a driving force for adsorption of the inhibitor on the mild steel surface. The value of ΔS_a increases in the presence of the inhibitor and is generally interpreted by increases in the disorder, as the reactants are converted to activated complexes [35].

2.4. Adsorption Isotherm

The adsorption isotherm was collected to investigate the interaction between the inhibitor and the mild steel surface. The surface coverage values (θ) were obtained from the polarization measurements and are calculated thus:

$$\theta = \frac{i_{\text{corr}}^0 - i_{\text{corr}}}{i_{\text{corr}}^0} \quad (9)$$

It was assumed that the adsorption of chlorocurcumin follows the Langmuir adsorption isotherm model. Plotting C_{inh}/θ against C_{inh} (Figure 7) resulted in a straight line, which indicates that the inhibitor adsorption obeys the Langmuir adsorption isotherm. The Langmuir adsorption isotherm is represented by Equation (10):

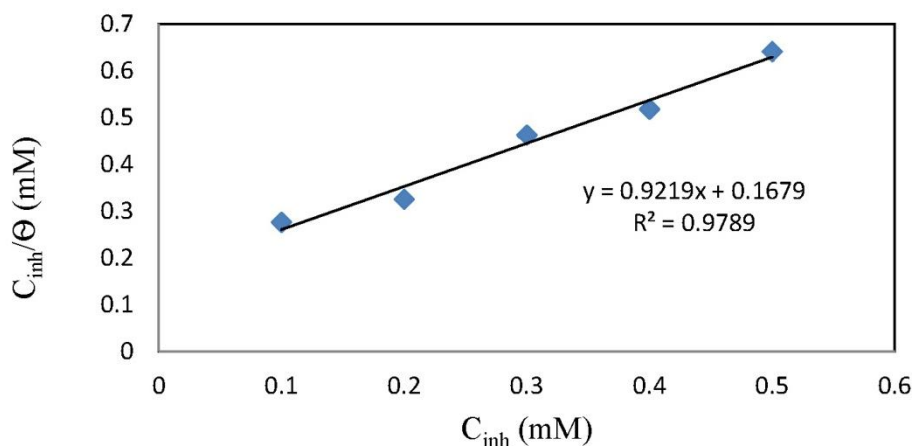
$$\frac{C_{\text{inh}}}{\theta} = \frac{1}{K_{\text{ads}}} + C_{\text{inh}} \quad (10)$$

where C_{inh} is the concentration of the inhibitor and K_{ads} is the adsorption constant that is related to the standard free energy of adsorption, ΔG_{ads}^0 as follow:

$$\Delta G_{\text{ads}}^0 = -RT \ln(55.5K_{\text{ads}}) \quad (11)$$

Generally, values of ΔG_{ads}^0 up to -20 kJ/mol are consistent with physisorption, while those approximately -40 kJ/mol or lower associated with chemisorption. Chemisorption involves charge sharing or charge transfer between the metal and organic molecules [36,37]. In this case, the calculated value for ΔG_{ads}^0 is -14.61 kJ/mol; the mechanism of adsorption for chlorocurcumin on mild steel is thus physisorption.

Figure 7. Adsorption isotherm for chlorocurcumin on the mild steel surface in 1.0 M HCl.



3. Experimental Section

All chemicals used were of reagent grade (supplied by either Malaysia|Sigma-Aldrich) and used as received without further purifications. The Fourier transform infrared (FTIR) spectra were measured using a Thermo Scientific Model Nicolet 6700 Spectrophotometer. NMR spectra were recorded on a Model AVANCE III 600 MHz spectrometer.

3.1. Synthesis of Chlorocurcumin

Curcumin (1.23 g, 0.00334 mol) was mixed with POCl_3 (10 mL). The resulting suspension was refluxed for approximately 3 hours, then cooled to room temperature and slowly poured onto crushed ice mixed with water. The violet solid formed was collected by filtration, washed with ice-water and recrystallized from acetonitrile. For the FTIR spectrum of chlorocurcumin, the broad peak at 3412.9 cm^{-1} was due to O–H stretching vibration while the sharp peak at 1727.8 was due to carbonyl

stretching. Both peaks at 2959.7 cm^{-1} and 2931.6 cm^{-1} were assigned to aromatic rings on chlorocurcumin. Peaks at 1598.8 cm^{-1} and 1513.0 cm^{-1} are the typical C=C stretch vibration. ^1H NMR (CDCl_3): δ (ppm) 7.5 (H=C=C); 7.27 (H-aromatic); 4.2 (–OH); 0.9 (–OCH₃). ^{13}C NMR (CDCl_3): δ (ppm) 167.7 (C=O); 128–132 (C-aromatic); 68.18 (C–Cl); 38.8(–OCH₃) [38].

3.2. Electrochemical Measurements

Mild steel specimens obtained from Metal Samples Company were used as the working electrodes throughout the study. The composition (wt %) of the mild steel was as follows: Fe, 99.21; C, 0.21; Si, 0.38; P, 0.09; S, 0.05; Mn, 0.05; Al, 0.01. The active surface area of the mild steel was 4.5 cm^2 . The specimens were cleaned according to ASTM standard procedure G1-03 [39–42]. The measurements were carried out in aerated, non-stirred 1.0 M hydrochloric acid solutions at 30, 40, 50 and 60 °C at a concentration range of 0.1–0.5 mM chlorocurcumin as the corrosion inhibitor. The selection of the acid concentration was based on the conditions commonly observed during the selection process at industrial facilities. Solutions were freshly prepared using distilled water. Each measurement was repeated three times, and only the average values were reported to verify the reproducibility of the experiments. The inhibitory effects of chlorocurcumin were investigated with a Gamry water jacketed glass cell, which contained three electrodes: the working, counter and reference electrode (the reference electrode consisted of a saturated calomel electrode (SCE)). The measurements were performed using a Gamry Instrument Potentiostat/Galvanostat/ZRA model REF 600.

4. Conclusions

Chlorocurcumin inhibits the corrosion of mild steel in 1.0 M HCl solution. The inhibition efficiency increases with the concentration of the inhibitor. Potentiodynamic polarization studies implied that the chlorocurcumin is a mixed-type inhibitor. The activation energy showed that the entire process is controlled by the polarization resistance, surface reaction and that the adsorption of chlorocurcumin on the metal surface obeyed the Langmuir adsorption isotherm.

Acknowledgements

The authors gratefully acknowledge the Universiti Kebangsaan Malaysia under the DIP-2012-02 grant.

Conflicts of Interest

The authors declare no conflict of interest.

References

1. Newman, D.J.; Cragg, G.M.; Snader, K.M. The influence of natural products upon drug discovery. *Nat. Prod. Rep.* **2000**, *17*, 215–234.
2. Myint, S.; Daud, W.R.W.; Mohamad, A.B.; Kadhun, A.A.H. Gas chromatographic determination of eugenol in ethanol extract of cloves. *J. Chromatogr. Biomed. Appl.* **1996**, *679*, 193–195.

3. Behpour, M.; Ghoreishi, S.M.; Gandomi-Niasar, A.; Soltani, N.; Salavati-Niasari, M. The inhibition of mild steel corrosion in hydrochloric acid media by two Schiff base compounds. *J. Mater. Sci.* **2009**, *44*, 2444–2453.
4. Tang, Y.M.; Yang, X.Y.; Yang, W.Z.; Wan, R.; Chen, Y.Z.; Yin, X.S. A preliminary investigation of corrosion inhibition of mild steel in 0.5 M H₂SO₄ by 2-amino-5-(n-pyridyl)-1,3,4-thiadiazole: Polarization, EIS and molecular dynamics simulations. *Corros. Sci.* **2010**, *52*, 1801–1808.
5. Cang, H.; Fei, Z.; Shi, W.; Xu, Q. Experimental and theoretical study for corrosion inhibition of mild steel by L-Cysteine. *Int. J. Electrochem. Sci.* **2012**, *7*, 10121–10131.
6. Kumar, H.; Karthikeyan, S. Inhibition of mild steel corrosion in hydrochloric acid solution by cloxacillin drug. *J. Mater. Environ. Sci.* **2012**, *3*, 925–934.
7. Wang, Z. The inhibition effect of bis-benzimidazole compound for mild steel in 0.5 M HCl solution. *Int. J. Electrochem. Sci.* **2012**, *7*, 11149–11160.
8. Ju, H.; Kai, Z.P.; Li, Y. Aminic nitrogen-bearing polydentate Schiff base compounds as corrosion inhibitors for iron in acidic media: A quantum chemical calculation. *Corros. Sci.* **2008**, *50*, 865–871.
9. El Issami, S.; Hammouti, B.; Kertit, S.; Addi, E.; Salghi, R. Triazolic compounds as corrosion inhibitors for copper in hydrochloric acid. *Pigment Resin Technol.* **2007**, *36*, 161–168.
10. Riggs, O.L., Jr.; Hurd, R.M. Temperature coefficient of corrosion inhibitor. *Corrosion* **1967**, *23*, 252–258.
11. Durnie, W.; Marco, R.D.; Jefferson, A.; Kinsella, B. Structure activity of oil field corrosion inhibitors. *J. Electrochem. Soc.* **1999** *146*, 1751–1756.
12. Bentiss, F.; Lebrini, M.; Lagrenée, M. Thermodynamic characterization of metal dissolution and inhibitor adsorption processes in mild steel/2,5-bis(n-thienyl)-1,3,4-thiadiazoles/hydrochloric acid system. *Corros. Sci.* **2005**, *47*, 2915–2931.
13. Oguzie, E.E.; Okolue, B.N.; Ebenso, E.E.; Onuoha, G.N.; Onuchukwu, A.I. Evaluation of the inhibitory effect of methylene blue dye on corrosion of aluminum in HCl. *Mater. Chem. Phys.* **2004**, *87*, 394–401.
14. Li, X.; Tang, L. Synergistic inhibition between OP and NaCl on the corrosion of cold-rolled steel in phosphoric acid. *Mater. Chem. Phys.* **2005**, *90*, 286–297.
15. Sinko, J. Challenges of chromate inhibitor pigments replacement in organic coating. *Prog. Org. Coat.* **2001**, *42*, 267–282.
16. Popova, A.; Christov, M. Evaluation of impedance measurements on mild steel corrosion in acid media in the presence of heterocyclic compounds. *Corros. Sci.* **2006**, *48*, 3208–3221.
17. Liu, F.G.; Du, M.; Zhang, J.; Qiu, M. Electrochemical behavior of Q235 steel in saltwater saturated with carbon dioxide based on new imidazoline derivative inhibitor. *Corros. Sci.* **2009**, *51*, 102–105.
18. Benabdellah, M.; Touzani, R.; Dafali, A.; Hammouti, M.; El Kadiri, S. Ruthenium–ligand complex, an efficient inhibitor of steel corrosion in H₃PO₄ media. *Mater. Lett.* **2007**, *61*, 1197–1204.
19. Bayol, E.; Gürten, A.A.; Dursun, M.; Kayakırlmaz, S. Adsorption behavior and inhibition corrosion effect of sodium carboxymethyl cellulose on mild steel in acidic medium. *Acta Phys. Chim. Sin.* **2008**, *24*, 2236–2242.

20. Popova, A. Temperature effect on mild steel corrosion in acid media in presence of azoles. *Corros. Sci.* **2007**, *49*, 2144–2158.
21. Li, W.; He, Q.; Zhang, S.; Pei, C.; Hou, B. Some new triazole derivatives as inhibitors for mild steel corrosion in acidic medium. *J. Appl. Electrochem.* **2008**, *38*, 289–295.
22. Ferreira, E.S.; Giacomelli, C.; Giacomelli, F.C.; Spinelli, A. Evaluation of the inhibitor effect of L-ascorbic acid on the corrosion of mild steel. *Mater. Chem. Phys.* **2004**, *83*, 129–134.
23. Larabi, L.; Harek, Y.; Traisnel, M.; Mansri, A. Synergistic influence of poly(4-vinylpyridine) and potassium iodide on inhibition of corrosion of mild steel in 1 M HCl. *J. Appl. Electrochem.* **2004**, *34*, 833–839.
24. Li, X.; Deng, S.; Fu, H. Benzyltrimethylammonium iodide as a corrosion inhibitor for steel in phosphoric acid produced by dihydrate wet method process. *Corros. Sci.* **2011**, *53*, 664–670.
25. Abo El-Khair, M.B.; Abdel Hamed, I.A. Thiosemicarbazide as an inhibitor for the acid corrosion of iron. *Corros. Sci.* **1976**, *16*, 163–169.
26. Shih, H.; Mansfeld, H. A fitting procedure for impedance data of systems with very low corrosion rates. *Corros. Sci.* **1989**, *29*, 1235–1240.
27. Elayyachy, M.; El Idrissi, A.; Hammouti, B. New thio-compounds as corrosion inhibitor for steel in 1 M HCl. *Corros. Sci.* **2006**, *48*, 2470–2479.
28. Jacob, K.S.; Parameswaran, G. Corrosion inhibition of mild steel in hydrochloric acid solution by Schiff base furoin thiosemicarbazone. *Corros. Sci.* **2010**, *52*, 224–228.
29. Prabhu, R.A.; Venkatesha, T.V.; Shanbhag, A.V.; Kulkarni, G.M.; Kalkhambkar, R.G. Inhibition effects of some Schiff's bases on the corrosion of mild steel in hydrochloric acid solution. *Corros. Sci.* **2008**, *50*, 3356–3362.
30. Fu, J.; Pan, J.; Liu, Z.; Li, S.; Wang, Y. Corrosion inhibition of mild steel by benzopyranone derivative in 1.0 M HCl solutions. *Int. J. Electrochem. Sci.* **2011**, *6*, 2072–2089.
31. Babic-Samardzija, K.; Khaled, K.F.; Hackerman, N. Heterocyclic amines and derivatives as corrosion inhibitors for iron in perchloric acid. *Anti Corros. Method. Mater.* **2005**, *52*, 11–21.
32. Shukla, S.K.; Quraishi, M.A.; Ebenso, E.E. Adsorption and corrosion inhibition properties of cefadroxil on mild steel in hydrochloric acid. *Int. J. Electrochem. Sci.* **2011**, *6*, 2912–2931.
33. Herrag, L.; Hammouti, B.; Elkadiri, S.; Aouniti, A.; Jama, C.; Vezin, H.; Bentiss, F. Adsorption properties and inhibition of mild steel corrosion in hydrochloric solution by some newly synthesized diamine derivatives: Experimental and theoretical investigations. *Corros. Sci.* **2010**, *52*, 3042–3051.
34. Boudalia, M.; Guenbour, A.; Bellaouchou, A.; Laqhaili, A.; Mousaddak, M.; Hakiki, A.; Hammouti, B.; Ebenso, E.E. Corrosion inhibition of organic oil extract of leaves of *lanvandula stoekas* on stainless steel in concentrated phosphoric acid solution. *Int. J. Electrochem. Sci.* **2013**, *8*, 7414–7424.
35. Musa, A.Y.; Mohamad, A.B.; Kadhum, A.A.H.; Takriff, M.S.; Lim, T.T. Synergistic effect of potassium iodide with phthalazone on the corrosion inhibition of mild steel in 1.0 M HCl. *Corros. Sci.* **2011**, *53*, 3672–3677.
36. Ell Quali, I.; Hammouti, B.; Aouniti, A.; Ramli, Y.; Azougagh, M.; Essassi, E.M.; Bouachrine, M. Thermodynamic characterisation of steel corrosion in HCl in the presence of 2-phenylthieno (3, 2-b) quinoxaline. *J. Mater. Environ. Sci.* **2010**, *1*, 1–8.

37. Musa, A.Y.; Kadhum, A.A.H.; Mohamad, A.B.; Takriff, M.S.; Daud, A.R.; Kamarudin, S.K. On the inhibition of mild steel corrosion by 4-amino-5-phenyl-4H-1, 2, 4-triazole-3-thiol. *Corros. Sci.* **2010**, *52*, 526–433.
38. Al-Amiery, A.; Kadhum, A.; Obayes, H.; Mohamad, A. Synthesis and antioxidant activities of novel 5-chlorocurcumin, complemented by semiempirical calculations. *Bioinorg. Chem. Appl.* **2013**, *2013*, 354982:1–354982:7.
39. Moretti, G.; Guidi, F.; Grion, G. Tryptamine as a green iron corrosion inhibitor in 0.5 M deaerated sulphuric acid. *Corros. Sci.* **2004**, *46*, 387–403.
40. American Society for Testing and Materials. Standard Practice for Preparing, Cleaning, and Evaluating Corrosion Test Specimens. Available online: http://www.cosasco.com/documents/ASTM_G1_Standard_Practice.pdf (accessed on 11 March 2013).
41. Al-amery, A.A.; Abdul, A.H.K.; Abu, B.M.; Sutiana, J. A novel hydrazinecarbothioamide as a potential corrosion inhibitor for mild steel in HCl. *Materials* **2013**, *6*, 1420–1431.
42. Junaedi, S.; Al-amery, A.; Kadhum, A.; Mohamad, A. Inhibition effects of a synthesized novel 4-Aminoantipyrine derivative on the corrosion of mild steel in hydrochloric acid solution together with quantum chemical studies. *Int. J. Mol. Sci.* **2013**, *14*, 11915–11928.

© 2013 by the authors; licensee MDPI, Basel, Switzerland. This article is an open access article distributed under the terms and conditions of the Creative Commons Attribution license (<http://creativecommons.org/licenses/by/3.0/>).